Geological Quarterly, 1999, **43** (4): 429–447

# History of sedimentation of the Nida Gypsum deposits (Middle Miocene, Carpathian Foredeep, southern Poland)

Maciej BĄBEL

Bąbel M. (1999) — History of sedimentation of the Nida Gypsum deposits (Middle Miocene, Carpathian Foredeep, southern Poland). Geol. Quart., **43** (4): 429–447. Warszawa.

The Nida Gypsum deposits are the best exposed in Poland part of the Middle Miocene (Badenian) evaporites of the Carpathian foreland basin. These deposits record various shallow water (< 5 m) evaporative environments. The facies sequence in the lower part of evaporites reflects shallowing (up to emersion) and than deepening accompanied with salinity rise up to halite precipitation. The salinity rise was arrested by refreshment promoting subaqueous dissolution of sodium chloride. This event was followed by the second large salinity rise and then final dilution of brine which finished evaporative sedimentation. The described two saline cyclothems are recognizable over large area of Carpathian foreland basin.

*Maciej Bąbel, Institute of Geology, Warsaw University, Żwirki i Wigury 93, PL-02-089 Warszawa, Poland; e-mail: babel@geo.uw.edu.pl*
*(received: June 9, 1999; accepted: September 20, 1999).*

Key words: Carpathian Foredeep, Badenian, depositional history, halite solution, cyclothems.

## INTRODUCTION

The Badenian Paratethyan salinity crisis led to deposition of evaporites in the marine Carpathian foreland basin. They are comprised of up to 60 m thick primary gypsum deposits exposed along the northern margin of the basin and 10–200 m thick clay-anhydrite-halite deposits buried near the Carpathian overthrust. The best exposed part of the sulphate evaporites in Poland — the Nida Gypsum deposits — are the subject of this paper (Fig. 1). These deposits, never deeply buried, show exceptionally well preserved primary depositional structures and are an excellent object for sedimentological studies over a period of many years (S. Kwiatkowski, 1972; L. Rosell *et al.*, 1998; M. Bąbel, 1999*b* and references therein).

The author aims to reconstruct the history of sedimentation of the Nida Gypsum deposits applying methodology of facies analysis. Facies of the Nida Gypsum deposits were defined and distinguished in the separate paper (M. Bąbel, 1999*b*) where their depositional environments were interpreted in detail. The depositional history presented here considers not only spatial distribution of these facies and associated sedimentary structures in outcrops and drill cores (M. Bąbel, 1992, 1999*b* with references therein) but also geochemical data (A. Kasprzyk, 1994; L. Rosell *et al.*, 1998). So far facies analyses of the Nida Gypsum deposits have only been briefly outlined by T. M. Peryt *et al.* (1994) and the present author (M. Bąbel, 1995, 1996*a*). The earlier facies studies by A. Kasprzyk (1991, 1993*a, b*) and B. Kubica (1992) were based on core materials from a much larger area of the foreland basin. The recognized sedimentary history of the Nida Gypsum deposits applies to the whole northern basin margin since the facies sequence is roughly the same in the area from the Czech Republic up to environs of Horodenka in Ukraine (B. Kubica, 1992; A. Kasprzyk, 1993*a*, 1995; T. M. Peryt, 1996; O. I. Petrichenko *et al.*, 1997; T. M. Peryt *et al.*, 1998; A. Roman, 1998; M. Bąbel, A. Boguckiy, 1999).

## GEOLOGICAL BACKGROUND

The Nida Gypsum deposits occur in two areas: the Pińczów and Wiślica area (Fig. 1; S. Kwiatkowski, 1974). The underlying pre-evaporitic Miocene deposits lie transgressive-

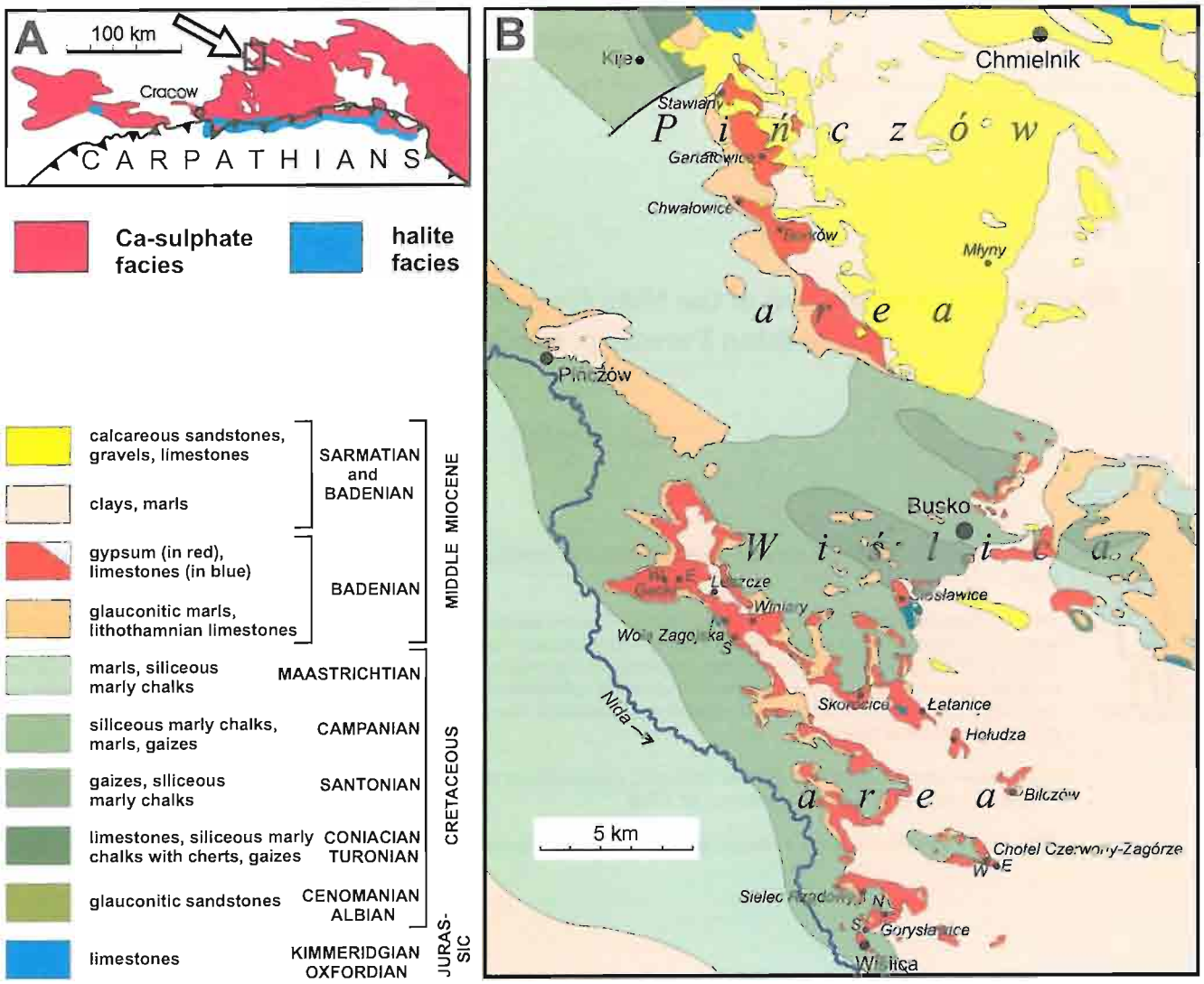


Fig. 1. Badenian (Middle Miocene) evaporites of southern Poland (**A**) and geologic map of the study area (**B**), without Pliocene and Quaternary cover; the Nida Gypsum deposits enclose Badenian carbonates shown in blue

ly on eroded Cretaceous and Jurassic substrate filling in depressions (A. Radwański, 1969). These marine deposits reach a maximum thickness of 115 m in the Pińczów area (at Młyny), and only some tens of metres in the Wiślica area where the evaporites commonly lie directly on the Cretaceous substrate. The evaporites are over 50 m thick in the Pińczów area (at Gartatowice, Stawiany) and are 34 m in thickness in the Wiślica area (at Gacki, Leszcze, Winiary; A. Wala, 1979). They are overlain by the Badenian–Sarmatian clays, marls and sandstones. The top of evaporites is commonly eroded and covered with the Quaternary clastics.

## DISTRIBUTION OF FACIES

Five primary facies of the Nida Gypsum deposits and their subfacies represent various evaporitic environments (Table 1; M. Bąbel, 1999*b*). Vertical facies sequence correlates well with the lithostratigraphic units of the Nida Gypsum deposits; layers lettered from **a** to **r** distinguished by A. Wala (1963, 1980) and lithosomes lettered from **A** to **G** by B. Kubica (1992). The giant intergrowth facies occurs only at the base of evaporites and it is overlain successively by the gypsum crystal debris facies (occurring locally at the boundary of lithosomes **A/B** or layers **a/b**; Fig. 2), the grass-like facies, the sabre facies, and the microcrystalline facies. The grass-like and the sabre facies appear also in the upper part of the section intercalating the microcrystalline gypsum (forming lithosome **F**, or layer **m**; Fig. 3).

Four thin marker beds (or specific parts of some beds) in the Nida Gypsum deposits were indicated by the author (M. Bąbel, 1996*a*) as chronohorizons recording isochronic events in the studied area (Figs. 2, 3). These chronohorizons form the stratigraphic framework for a sedimentological interpretation. The vertical facies sequence reflects the general history

Table 1

**Facies of the Nida Gypsum deposits and their inferred sedimentary environments**

| Facies | Subfacies | Illustrations | Inferred depositional environment |
|---|---|---|---|
| Microcrystalline gypsum | Breccias | Pl. IV, Fig. 1<br>Pl. V; Pl. VI, Fig. 1 | Density stratified saline pan with salinity fluctuating at the halite saturation level and calcium depleted sulphate brine |
| | Alabasters | | |
| | Laminated gypsum | | |
| Sabre gypsum | Wavy bedded | Pl. III, Fig. 1 | Density stratified saline pan with calcium sulphate saturated brine of high salinity |
| | Flat bedded | Pl. III, Figs. 1, 2 | |
| Grass-like gypsum | Subfacies with crystal rows | Pl. II, Fig. 2 | Semi-emerged evaporitic shoal with selenitic banks and shallow saline pans (filled with calcium sulphate saturated brine) passing into coastal clay-gypsum flat |
| | Alabaster beds subfacies | Pl. II, Fig. 2 | |
| | Stromatolitic domes subfacies | | |
| | Subfacies with clay intercalations | Pl. II, Fig. 2 | |
| Gypsum crystal debris | | Pl. I, Figs. 1, 2 | Semi-emerged clay-gypsum (sabkha-like) flat |
| Giant gypsum intergrowths | Non-palisade intergrowths | | Density stratified saline pan with calcium sulphate saturated brine of low salinity |
| | Palisade intergrowths (skeletal and massive) | Pl. I, Figs. 1, 2 | |
| | Clay subfacies | | |

of sedimentation. Lateral subfacies transitions are used to reconstruct palaeogeography.

## SEDIMENTATION OF THE NIDA GYPSUM DEPOSITS

### ONSET OF EVAPORATION

Before deposition of the discussed evaporites the Carpathian foreland basin was a fully marine part of Paratethys. It has been commonly assumed that the evaporative deposition in this basin was caused by reduction of its connections with the Mediterranean (e.g. A. Radwański, 1969; S. Kwiatkowski, 1972; A. Garlicki, 1979; F. Rögl, F. F. Steininger, 1984). A global sea level drop and possible cooling of climate were also suggested as causes of evaporation (J. Szczechura, 1982; G. Demarcq, 1989; N. Oszczypko, 1996, 1998).

Excess of regional evaporation over a water influx into the basin promoted a gradual salinity increase. The more saline and dense waters flowed down and collected within basinal depressions. These denser waters became resistant to a vertical circulation. Their oxygenation gradually dropped because the rate of oxygen consumption was higher than the rate of supply. In the northern part of the foreland basin the *Ervilia* coquina represents this pre-evaporitic stage inhospitable for most marine organisms (A. Radwański, 1969; S. Kwiatkowski, 1972). This cocquina contains abundant but species-depleted fauna, almost exclusively composed of two mollusc species: *Modiola hoernesi* Reuss and *Ervilia pusilla* Philippi. They flourished because of their particular adaptation to an increased salinity and low oxygenation (K. Kowalewski, 1966). In the studied area the *Ervilia* cocquina (0.1–10 cm thick) occurs only locally and contains authigenic glauconite. It is covered with up to 20 cm thick black bituminous clays.

Due to the high rate of evaporation and salinity increase a density stratification was established in the northern area of the foreland basin (having a depth of several metres). More dense water was accumulated below the pycnocline and its salinity continuously rose.

### SULPHATE DEPOSITION (LITHOSOMES A–D)

#### STRATIFIED SULPHATE BRINE OF LOW SALINITY (LITHOSOME A)

The bottom brines first reached the phase of gypsum precipitation. Within the upper part of water body a salinity was still too low for gypsum precipitation. In such several metres deep density-stratified brines the giant gypsum intergrowths were deposited thus beginning the sulphate succession. The intergrowths started to grow as isolated aggregates in the deeper and weakly oxygenated Pińczów area and commonly developed as continuous crusts with palisade structure in the Wiślica area (Pl. I, Fig. 2; M. Bąbel, 1999*b*, fig. 3). Further growth led to development of the palisade structure in the whole area. The deposition rate was slower in the Wiślica area where dissolution surfaces are more common and coeval growth zones of crystals within chronohorizon A are thinner than in the Pińczów area (Fig. 2; M. Bąbel, 1987, pl. 3, fig. 1).

#### SULPHATE EVAPORITIC SHOAL (LITHOSOME B)

Shallowing and emersion arrested the growth of giant intergrowths. Dissolution surfaces, which are more frequent to the top of giant crystal layer, record a gradual shallowing.

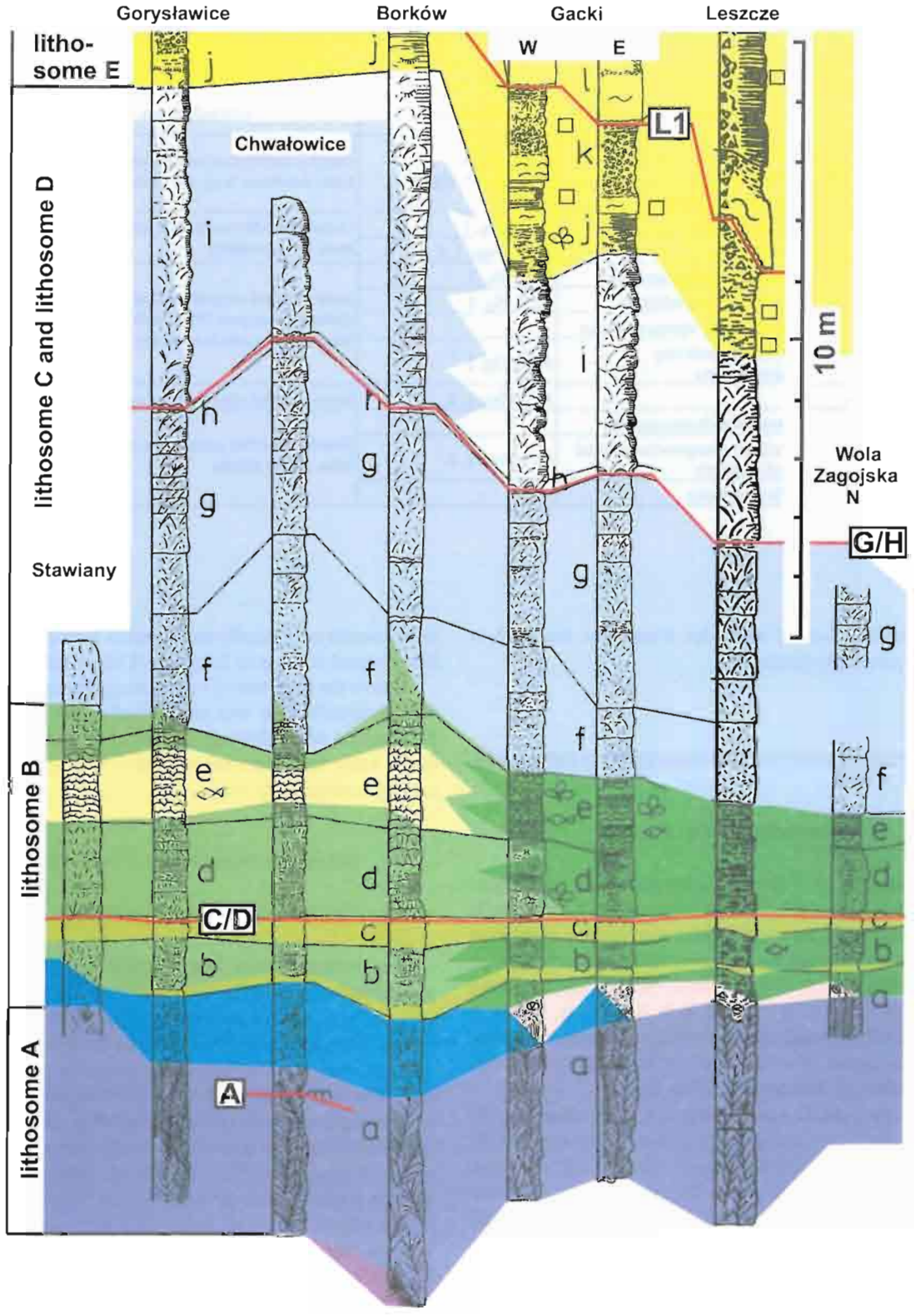


Fig. 2. Lithology, stratigraphy and facies of the lower part of Nida Gypsum deposits (see Fig. 1B for section localities)

1–3 — giant gypsum intergrowths: 1 — clay subfacies, 2 — palisade subfacies, 3 — non-palisade subfacies; 4 — gypsum crystal debris; 5–8 — grass-like gypsum: 5 — subfacies with clay intercalations, 6 — subfacies with alabaster beds, 7 — subfacies with stromatolitic domes, 8 — subfacies with crystal rows; 9, 10 — sabre gypsum: 9 — flat bedded subfacies, 10 — wavy bedded subfacies; 11 — microcrystalline gypsum; 12 — aggregated gypsum crystals and intergrowths placed in clay; 13 — giant gypsum intergrowths with palisade structure; 14 — correlable crystal growth zonation; 15 — dissolution surfaces within palisade intergrowths; 16 — giant gypsum intergrowths with non-palisade structure; 17 — broken, abraded and corroded gypsum crystals; 18 — grass-like gypsum crystals intercalating alabaster beds; 19 — stacked rows of grass-like gypsum crystals; 20 — clay and clayey gypsum; 21 — microbial gypsum domes

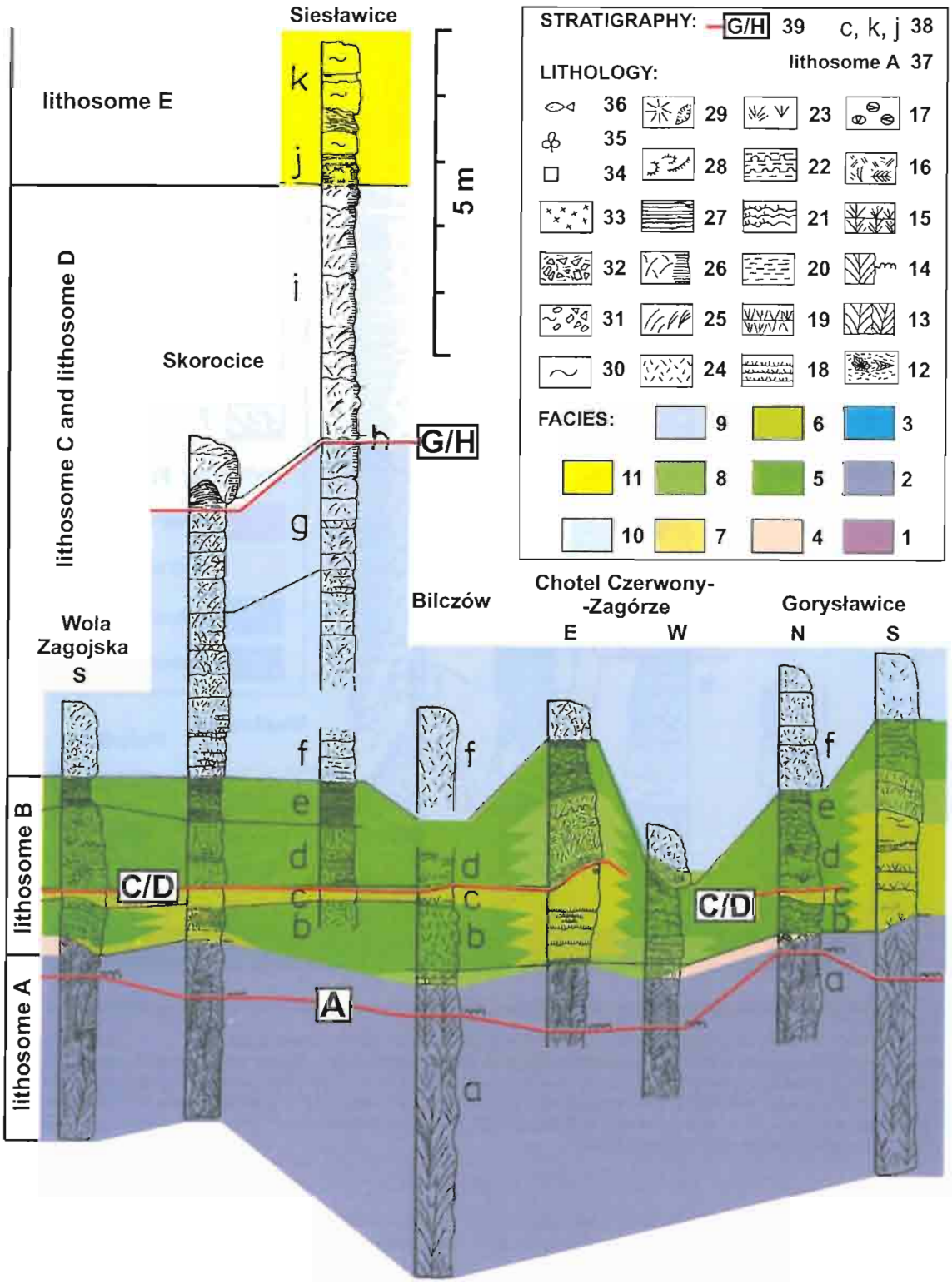


(right) overgrown with grass-like crystals (left); 22 — microbial alabaster domes intercalated with clay; 23 — fan-like aggregates of grass-like crystals; 24 — rod-like gysum crystals < 15 cm long; 25 — sabre gypsum crystals > 15 cm long (left) and their aggregates (right); 26 — sabre gypsum crystals within laminated gypsum; 27 — flat and wavy laminated gypsum; 28 — arcuate and elliptical aggregates of gypsum crystals (see S. Kwiatkowski, 1972); 29 — radial (left) and drusy (right) aggregates of gypsum crystals; 30 — compact fine-grained gypsum ("alabaster"): banded, spoted and with relic lamination (see S. Kwiatkowski, 1972); 31 — gypsum breccias with "alabaster" matrix; 32 — gypsum breccias with clay matrix; 33 — gypsum porphyroblasts and their aggregates; 34 — traces after halite crystals; 35 — floral remains; 36 — fish remnants; 37 — lithosomes after B. Kubica (1992); 38 — layers lettered after A. Wala (1979, 1980); 39 — chronohorizons after M. Bąbel (1996*a*)

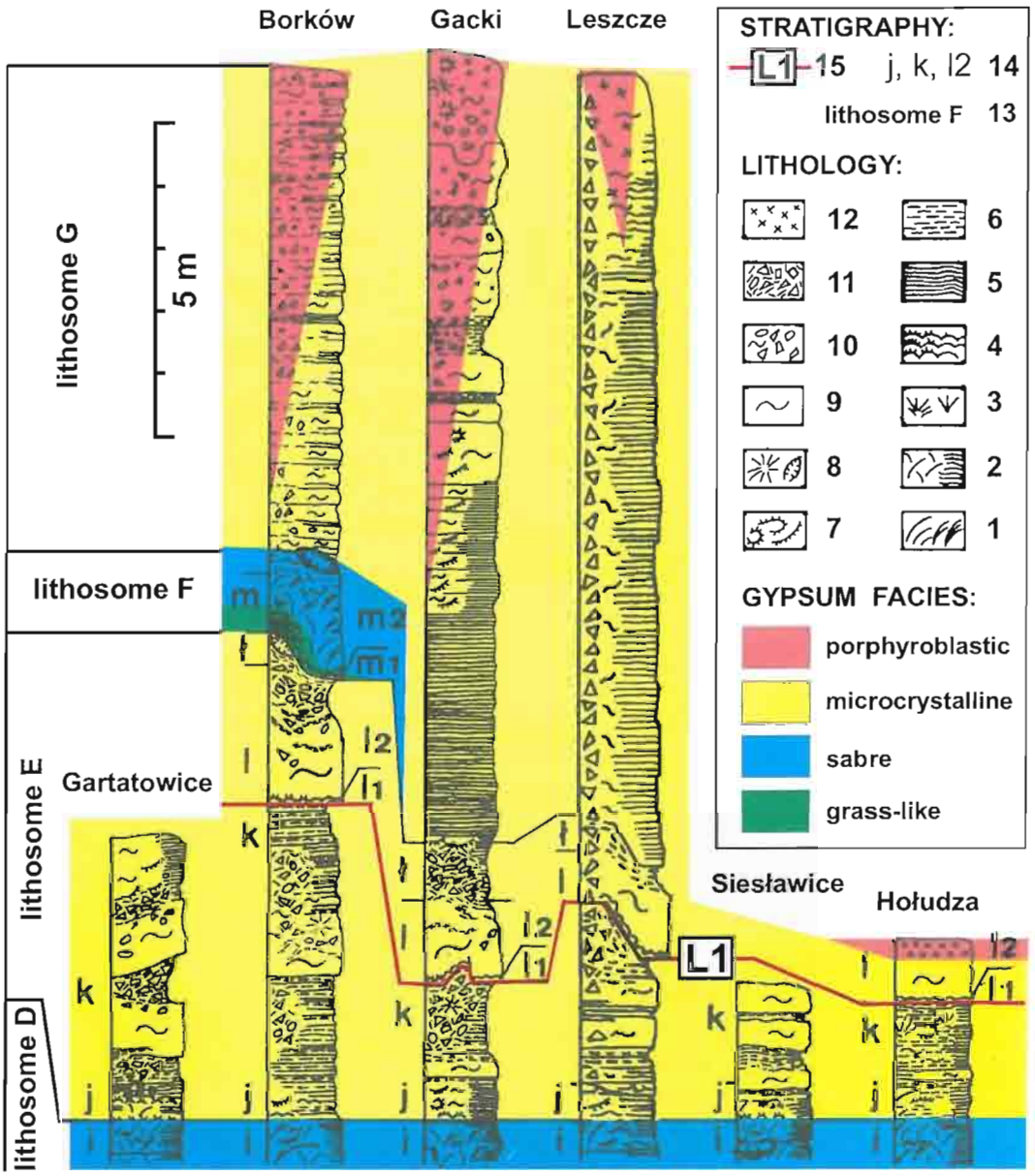


Fig. 3. Lithology, stratigraphy and facies of the upper part of the Nida Gypsum deposits (see Fig. 1B for section localities)

1 — sabre gypsum crystals (left) and their aggregates (right); 2 — sabre gypsum crystals within laminated gypsum; 3 — fan-like aggregates of grass-like gypsum crystals; 4 — microbial gypsum domes (right) overgrown with grass-like crystals (left); 5 — flat and wavy laminated gypsum; 6 — clay and cleyey gypsum; 7 — arcuate and elliptical aggregates of gypsum crystals (see S. Kwiatkowski, 1972); 8 — radial (left) and drusy (right) aggregates of gypsum crystals; 9 — compact fine-grained gypsum ("alabaster"); 10 — gypsum breccias with "alabaster" matrix; 11 — gypsum breccias with clay matrix; 12 — gypsum porphyroblasts and their aggregates; 13 — lithosomes after B. Kubica (1992); 14 — layers lettered after A. Wala (1979, 1980), supplemented and modified (M. Bąbel, 1991); 15 — chronohorizons after M. Bąbel (1996*a*)

Brine dilution by meteoric water input and, consequently, gypsum dissolution was easier in the shallow basin (*cf.* J. K. Warren, 1982). Growth of giant crystals was replaced by deposition of grass-like gypsum of lithosome **B** representing a shallow evaporitic flat.

In the Wiślica area gypsum crystal debris, covering the intergrowths (Pl. I, Figs. 1, 2), is evidence for a period of emersion supposedly connected with slight uplift of that area (M. Bąbel, 1999*b*, fig. 4). Simultaneously, on the submerged or only episodically emerged Pińczów area the non-palisade facies was deposited in a shallow brine (Fig. 2). The southern part of these evaporitic flats was supplied with clay carried by sheet-flood from land located south of Wiślica and Gacki (M. Bąbel, 1999*b*, fig. 6). An evaporitic clay-gypsum flat was developed over the crystal debris in the Wiślica area except for its highest elevations where flourishing microbial mats underwent gypsification, partly in a sabkha-like environment. Such areas are represented by rare subfacies with alabaster beds (Fig. 2; M. Bąbel, 1999*b*, fig. 6) directly covering the giant intergrowths (Pl. II, Fig. 2). On slopes of such elevated

areas thick massive rows of grass-like crystals grew commonly as scattered domal or platformal forms. At the same time the Pińczów area was a shallow saline pan isolated from clay supply. Large rows of grass-like crystals grew in a density stratified brine on its bottom, alternately with deposition of microbial gypsum during periods of lower salinity.

During deposition of the marker layer **c** (Fig. 2) brine properties were roughly the same in the whole northern part of the foreland basin which showed extremely flat relief (M. Bąbel, A. Boguckiy, 1999). Climatically controlled microbial deposition took place in a very shallow, saline brine. The 40–30 cm thick alabaster layer **c** thins up towards the south and disappears near Chotel Czerwony and Wiślica (Fig. 2) due to subaerial exposure of this area and nondeposition, or later erosion. It is absent at environs of Czarkowy, several kilometres south-east of Wiślica, because this part of basin was emerged since the onset of evaporation (T. Osmólski, 1972). Episodic emersion (A. Kasprzyk, 1993*a*) or climatically controlled refreshment stopped the microbial gypsum deposition. Sheet floods deposited clay on the top surface of layer **c** across the whole foreland basin (M. Bąbel, A. Boguckiy, 1999). Environs of Wiślica were a temporarily emerged sulphate sabkha at that time as indicated by nodular and brecciation structures in alabaster layer **c** from that area.

After these events the evaporative sedimentation still continued with the same environmental pattern: within a shallow saline pan in the Pińczów area and on a clay-gypsum flat or shoal in the Wiślica area (M. Bąbel, 1999*b*, fig. 6). During deposition of layer **e** (Fig. 2) the saline pan in the Pińczów area probably opened towards deeper brine body. As a result, wind waves and currents became very common in this area. At the same time frequent rains promoted numerous floods in the Wiślica area. The resulting peculiar biotic and dynamic conditions led to accretion of spectacular gypsum stromatolites (Fig. 2; M. Bąbel, 1999*b*).

## STRATIFIED SULPHATE BRINE OF HIGH SALINITY (LITHOSOMES C AND D)

Sedimentation on the large evaporite shoal was arrested by progressive basin deepening. The basin returned to a relatively constant density stratification. Continuous syntaxial bottom growth of large gypsum crystals was again (after the giant intergrowths) the main mechanism of sulphate deposition and this time produced the sabre gypsum deposits of lithosomes **C** and **D** (Fig. 2). However, morphology of bottom-grown crystals changed due to progressive salinity rise and associated modification of brine composition and lowered oxygenation (M. Bąbel, 1994; L. Rosell *et al.*, 1998).

In the Pińczów area the deepening of a shallow saline pan was gradual. Grass-like crystals grew as thicker and more thicker rows formed not only by single generation of individuals but by crystals grown one on the other. They gradually created thicker layers of sabre gypsum (Pl. III, Fig. 2). Simultaneously deposition of microbial gypsum decreased. In the Wiślica area the environmental change was more drastic and associated with a rapid restriction of clay-supplying sheet flood deposition. The clay-gypsum coastal flat together with adjacent land were flooded by saline waters and density stratification was re-established in a relatively deep brine. Hence sabre gypsum was deposited directly on the clay-rich substrate (Pl. II, Fig. 2), especially in former depressions of the flat. Only in some elevated areas uncovered with clay, the facies transition was gradual and connected with development of giant domal structures common in environs of Wiślica (Pl. II, Fig. 1). They occur in clusters, one near the other, passing laterally into a flat or wavy bedded sabre gypsum which formed in adjacent depressions (M. Bąbel, 1999*b*, fig. 7). The southern part of the Wiślica area was more shallow and sabre crystals were commonly dissolved there by meteoric waters (M. Bąbel, 1999*b*, pl. VIII, fig. 2). The discussed sabre gypsum layers gradually thin up toward the southern and southeastern emergent areas (Fig. 2; A. Wala, 1979; T. Osmólski, 1972).

The sabre gypsum deposition was interrupted by a short period of climatically controlled dilution of brine by meteoric waters and local emersion during deposition of layer **h** (Fig. 2; Pl. III, Figs. 1, 2). This event was similar to that recognized at the top of layer **c**. Sheet floods covered the hard rocky top of layer **g** with clay and clastic gypsum in nearly the whole margin of foreland basin (A. Kasprzyk, 1993*a, b*; T. M. Peryt, 1996).

Following deposition of the wavy bedded sabre subfacies layer **i** (in the Wiślica area; Fig. 2; Pl. III, Fig. 1) was connected with the important basin-wide environmental change which, as discussed in the next chapter, led to abundant precipitation of a very tiny gypsum crystals. The sabre crystals grew together with settling of such tiny crystals from the brine column. This fine-grained gypsum was commonly deposited in the Wiślica area where the wavy bedded subfacies was typically developed and locally comprises nucleation cones (*sensu* H. Dronkert, 1985). The bottom-grown sabre crystals were involved in various types of soft-sediment deformation. They included load structures below the sabre crystals, typical of nucleation cones, slumps, debris flows, and very common gravity creep of sabre crystals "floating" within the fine-grained gypsum matrix. At the same time the sabre crystals accreted as even beds intercalated with fine-grained gypsum in the Pińczów area (Fig. 2; Pl. III, Fig. 2). It seems that the brine there was more oxygenated and shallow than in the Wiślica area, or possibly only less saline (L. Rosell *et al.*, 1998). Geochemical evidences from other parts of the basin suggest a general slight brine dilution at that time (L. Rosell *et al.*, 1998).

During the sabre gypsum deposition the salinity was higher than at the time of the giant intergrowth crystallization (M. Bąbel, 1994). This is proved by increase in a strontium content within the bottom-grown gypsum crystals from 0.13% in the giant intergrowths up to 0.45% in layer **g** and 0.54% in layer **i** (A. Kasprzyk, 1994, fig. 2), similarly to gypsum crystals from many modern salinas (L. Rosell *et al.*, 1998).

In the stratigraphic accumulation from layer **f** to **i** the crystal size increases and particularly the sabre crystals (> 0.2 m long) are more frequent and larger (Fig. 2). This is interpreted to result from a gradual rise both of salinity and increasing depth of brines. In recent salinas the largest crystals commonly grew in the middle phase of gypsum precipitation (D.

Geisler-Cussey, 1986). On the other hand the permanently stratified, several metres deep brines favour the growth of large crystals (J. K. Warren, 1982). In shallow salinas, at a depth up to *ca.* 1 m, only several centimetres long crystals grow together with abundant gypsum sand representing gypsified organic mats accreting in photic zone (F. Ortí Cabo *et al.*, 1984; D. Geisler-Cussey, 1997). J. K. Warren (1982) reported the palisade growth of large decimetric gypsum crystals also in a shallow (at minimum depth 30 cm) saline pan within permanently subaqueous conditions. The palisade crystals show growth zonation created by strips of carbonate pellets horizontally cross-cutting their bodies. This zonation resulted from repeated dissolution (due to seasonal refreshments) and crystal regrowth. Such horizontal zonation was never noticed in the sabre crystals which commonly show perfect 120 growth zones without any traces of rounding and corrosion. Lack of such dissolution features in sabre crystals indicates that they grew at depths not available for surficial diluted waters.

### TRANSITION FROM SULPHATE TO SULPHATE-CHLORIDE SEDIMENTATION (LITHOSOMES D AND E)

Transition between the sabre and microcrystalline facies (between layers **i** and **k** or, roughly, between lithosome **D** and **E**; Figs. 2, 3) is associated with a change in mechanism of gypsum deposition (M. Bąbel, 1999*b*, fig. 2) recorded in the whole Carpathian foreland basin (T. M. Peryt, 1996; L. Rosell *et al.*, 1998). The gypsum crystallization directly on the bottom (in layer **g**) was gradually limited (in layers **i** and **j**) and entirely replaced by mechanical deposition: precipitation and fallout of tiny gypsum crystals within the brine column and/or their redeposition (in layer **k** and in the upper part of evaporites). This change was accompanied with the onset of halite crystallization, just at the base of layer **k**, continuing in nearly the whole section above (M. Bąbel, 1996*a*, tab. I). The discussed transition was variously explained by previous authors which commonly suggested some drastic change in basin anatomy and chemistry of brine (T. M. Peryt, 1996; A. Kasprzyk, 1997; L. Rosell *et al.*, 1998).

M. Pawlikowski (1982) supposed that in the course of evaporation volume of bottom highest salinity brines has increased to such a degree that the pycnocline rose to the water surface and gypsum precipitation took place within the whole brine volume. However, this does not explain the lack of bottom-grown gypsum crystals in the microcrystalline facies.

M. Bąbel (1995, 1996*a*) suggested that due to prolonged density stratification the oxygenation of stagnating bottom brines gradually diminished and amount of $SO_4^{2-}$ ions necessary for gypsum precipitation decreased, destroyed by sulphate reducing bacteria (P. Sonnenfeld, 1984). This process inhibited the gypsum growth at the sediment-brine interface (but not within the lighter surficial, oxygenated brines; M. Bąbel, 1996*a*, fig. 27). The deposition of laminated gypsum in an anoxic environment was earlier suggested by S. Kwiatkowski (1972) and J. Niemczyk (1985, 1988).

The other probably the most important reason for the stop of gypsum precipitation at the bottom was a calcium deficit (M. Bąbel, 1999*a*). If basinal brines are marine and close to the halite precipitation phase, they become significantly depleted in Ca ions being nearly totally fixed within the gypsum precipitate (P. Sonnenfeld, 1984).

The discussed transition is thus interpreted as a result of gradual and long-term evolution of brine towards the halite saturation level and nearly total depletion of Ca ions. The ensuing density rise of bottom brine led to the lowering of its oxygen and sulphate ion content (due to bacterial sulphate reduction as well as lowered solubility of oxygen in the highly saline brine; P. Sonnenfeld, 1984). The brine reached a transitional state between halite and gypsum precipitation characteristic for sedimentation of microcrystalline facies.

The wavy bedded sabre subfacies layer **i** (Figs. 2, 3) represents gradual inhibition of the gypsum crystallization at the bottom (reflecting progressively lowering concentration of $Ca^{2+}$ and/or $SO_4^{2-}$ within the bottom brine), and more intensive precipitation of this mineral within the better oxygenated and enriched in $SO_4^{2-}$ brines located closer to a brine-air interface.

### SULPHATE-CHLORIDE DEPOSITION (LITHOSOMES E AND G)

#### STRATIFIED SULPHATE-CHLORIDE BRINE OF HIGH AND FLUCTUATING SALINITY

During evaporative sedimentation at the boundary of layers **j** and **k** the calcium sulphate brine, previously crystallizating only gypsum, has evolved into Ca depleted sulphate-chloride brine with salinity fluctuating at the onset of the halite precipitation phase. The whole section above layer **j** is dominated by microcrystalline facies recording the newly established conditions of mixed sulphate-chloride sedimentation (Fig. 3). Because of the appearance of highly dense, halite-saturated brine the basin obtained more complex density stratification than before; with anoxic chloride brine at the bottom and oxygenated sulphatic brine above (M. Bąbel, 1996*a*). During deposition of microcrystalline (laminated) facies halite crystals grew within the anoxic brine directly at the basin floor while within oxygenated and hence richer in sulphates brines above, the tiny gypsum crystals still precipitated and sank to the bottom. The precipitation of gypsum was not only a result of Ca-sulphate concentration rise due to removal of $H_2O$ by evaporation, but also a consequence of brine mixing (M. Bąbel, 1999*a*). The precipitation was promoted by influxes of lower salinity $Ca^{2+}$ and $SO_4^{2-}$ rich brines flowing in from other parts of foreland basin, probably from the east, as suggested by general pattern of brine flow in the basin (S. Połtowicz, 1993; M. Bąbel *et al.*, 1999). The gypsum precipitated at the contact of mixing brines with different salinities, i.e. mainly along a pycnocline (M. Bąbel, 1999*a*), as it is sometimes observed in recent salinas (L. Rosell *et al.*, 1998) and in laboratories (O. B. Raup, 1982).

Redeposited gypsum, common in the microcrystalline facies, is a product of described complex brine stratification and composition of pore brines within the bottom sediments. The redeposition resulted from a lack of bottom crystal-

lization of gypsum necessary for cementation of surficial sediments (owing to the low concentration of $Ca^{2+}$ and $SO_4^{2-}$). Because of the lack of cementation the accumulating gypsum remained loose and soft, and hence it was easily subjected to winnowing and gravity redeposition even on slightly inclined slopes (M. Bąbel, 1999*a*). The other possible reason for redeposition was tectonically induced destruction of marginal gypsum sediments and their gravitational transport into subsiding depressions (B. Kubica, 1992; T. M. Peryt, A. Kasprzyk, 1992; J. Niemczyk, 1994, 1995, 1996*a–c*, 1997; T. M. Peryt, M. Jasionowski, 1994; T. M. Peryt, 1996).

The stratified saline water body underwent fluctuations either because of influx of meteoric waters or less saline brines from other parts of the basin. This led to salinity oscillations around the beginning of halite saturation phase. During salinity falls the bottom-grown halite was dissolved both directly at the bottom and under a cover of fine-grained gypsum. In the latter case residual alabasters were formed. They are common in layers **k**, **l2** and in the whole upper part of the gypsum succession (Fig. 3).

During phases of chloride sedimentation, thicker halite-rich strata were deposited (as recognized first by K. Kowalewski (1957) at the environs of Tarnobrzeg). They were all later completely dissolved both during and after evaporative sedimentation. The halite leaching was gradual and long-termed and it commonly led to multiple events of various scale solution-collapse and solution-subsidence deformation.

It is difficult to estimate how thick the halite-bearing strata were originally. Abundance of solution residual deposits and breccias and occurrence of relic chloride brines after halite solution (exploited at Busko Spa, A. Zuber *et al.*, 1997) prove that the original amount of halite was significant. In the Wiślica area, at Leszcze and Gacki, two thicker strata of post-halite residual alabasters and solution-collapse breccias are present within laminated gypsum in layer **k** (Fig. 3; Pl. V). Such strata are unrecognizable in the Pińczów area where, at Borków and Gartatowice, the whole layer **k** is strongly disturbed by halite solution (Pl. VI, Fig. 1). Substantial amounts of halite were also present within layer **ł** and in the top part of the evaporites (M. Bąbel, 1991, 1996*b*).

Relics after halite appear in the almost whole upper part of the gypsum succession indicating that the sulphate-chloride sedimentation continued to the end of the evaporative deposition. This deposition was interrupted during sedimentation of exclusively sulphatic layers **l1** and **m**, which do not show traces of halite but, instead, contain evidence of gypsum precipitation directly on the bottom (Fig. 3). Several larger influxes of meteoric waters, as recorded by clay intervals in layers **k** and **ł** and in the top parts of gypsum sections (A. Wala, 1979), disturbed evaporative deposition.

The layer **l1**, composed of 6 cm thick laminated domal microbial gypsum, locally with small bottom-grown sabre crystals, represents the short-term re-appearance of Ca-sulphate saturated brines on the basin floor. The early cementation transformed the layer **l1** (unlike the under- and overlain sediments) into a hard crust covering the whole bottom surface.

The layer **m** represents a large scale dilution event described separately below.

## REFRESHMENTS AND RETURNS OF SULPHATE DEPOSITION (LITHOSOME F AND ASSOCIATED STRATA)

The halite deposits in layer **k** at Gacki and Leszcze were totally dissolved after sedimentation of more than 10 m thick cover of gypsum deposits, as evidenced by the extent of collapse breccias and solution-subsidence deformation (Pl. IV, Fig. 1; Pl. V). However, the dissolution of these halite deposits probably started earlier, during salinity falls in the course of evaporative sedimentation, as it has been recognized in the Pińczów area (M. Bąbel, 1996*b*). The main reason of this diagenetic dissolution was both an upward and downward ionic diffusion of sodium chloride in pore waters (M. Bąbel, 1991, 1996*a*). The dissolution was facilitated by movements of pore brines promoted by initial solution-brecciation of sediments (T. M. Peryt, M. Jasionowski, 1994).

Extent and character of solution-related deformation at Borków suggest two events of subaqueous halite dissolution from layers **k** and **ł**. The dissolution probably began immediately after deposition of these layers and finished at the end of deposition of the covering layers **l1** and **m**, which both show flat undisturbed top surfaces (Pl. VI, Fig. 1; M. Bąbel, 1996*b*). It is possible that the dissolution only slowed at these moments and the remaining halite was leached later without significant deformation of the overlying strata. The dissolution events were caused by two larger salinity falls at the boundaries of **k/l1** and **ł/m**. These events coincide with influx of marine pteropods and foraminifera, typical of normal salinity water, in the same interval, i.e. within lithosome **E**, in the other areas of the basin, particularly between Szydłów and Stalowa Wola (E. Odrzywolska-Bieńkowa, 1975; B. Kubica, 1985, 1992; A. Kasprzyk, 1989; T. M. Peryt *et al.*, 1994). The abundant and well preserved marine fauna was found in clays intercalated gypsum also in the Czech Republic (T. M. Peryt *et al.*, 1997) and Ukraine (L. C. Pishvanova, 1963; V. A. Prisyazhniuk *et al.*, 1997). Thus it seems that refreshment was promoted by influx of marine waters. On the other hand a significant clay input is recorded in the whole basin within lithosome **E** (B. Kubica, 1992; S. Połtowicz, 1993) suggesting large influx of clay loaded meteoric waters and thus climatic control of these refreshments.

The brine dilution at the boundary **ł/m** (at the base of lithosome **F**) was the largest. During this event the brine properties and structure of brine column returned to its former state, i.e. characteristic for deposition of grass-like gypsum in lithosome **B**. The salinity fell at least to the beginning of gypsum precipitation phase. The ensuing salinity rise led first to deposition of grass-like and then sabre gypsum in layers **m1** and **m2** (both composing lithosome **F**). The gypsified organic mats of layer **m1** (Pl. IV, Fig. 2) again represent salinity oscillations at the beginning of gypsum precipitation phase (M. Bąbel, 1999*b*). Such brine was undersaturated with NaCl and thus able to dissolve halite from bottom sediments of layer **ł** (M. Bąbel, 1996*b*). The irregular base of layer **m** (Pl. VI, Fig. 1) is a product of a post-depositional subsidence and sediment collapse into hollows after leaching halite (M. Bąbel, 1991). Lenticular druse or geode-like bodies of centripetally-grown gypsum crystals found both below the base of layer **m** and within that layer (Fig. 3; Pl. VI, Fig. 2; T. M. Peryt, M. Jasionowski, 1994, fig. 5) represent infillings of

large shelter cavities which opened above zones of dissolving halite (M. Bąbel, 1996*b*). Such cavities were roofed by rigid crusts of bottom-grown gypsum crystals in layer **m**. Flat top of that layer is covered with microcrystalline gypsum with abundant halite traces. This suggests that solution-subsidence was stopped just after deposition of layer **m** because the brine again attained halite saturation.

The described event, a refreshment followed by a rapid salinity rise, is recorded in the whole northern margin of the basin by widespread, thin (0–4 m) lithosome **F** sandwiched within the layers of microcrystalline gypsum (B. Kubica, 1992; A. Kasprzyk, 1995; T. M. Peryt, 1996). The author's observations in Ukraine suggest that emersion preceded deposition of lithosome **F** there. The shallowing or emersion seems possible also in the studied area but clear evidences for it, or against it, are absent or obscured by halite dissolution.

During the discussed events the Pińczów area was probably more shallow than the Wiślica one and there was a salinity gradient between them. The layer **k** at Borków locally contains intercalations of grass-like gypsum with thin crusts and patches of bottom-grown gypsum crystals (subfacies with clay intercalations). This suggests a very shallow environment typical of evaporitic shoal deposition (M. Bąbel, 1999*b*). The mentioned subfacies was not recorded in layer **k** in the Wiślica area, probably because of its deeper and/or more saline depositional environment. Gypsified organic mats in layer **m1** (Pl. IV, Fig. 2) represent environment of such an evaporitic shoal (< 1 m deep). This layer (together with sabre gypsum layer **m2**) occurs in the Pińczów area (Fig. 3) and locally at Gacki in the Wiślica area (A. Wala, 1979). In the latter area layers **m1** and **m2** seem to pass laterally into microcrystalline gypsum (covering layer **ł**) which represent a deeper and anoxic or probably only more saline brine inhibiting the bottom crystallization of gypsum. Probably due to presence of such highly saline brines there, the halite in layers **k** and **l2–ł** was not dissolved completely during the salinity fall at the boundary of layers **ł–m** but later, after evaporative deposition.

### END OF EVAPORATIVE SEDIMENTATION

Evaporative deposition was arrested by a final marine refreshment of brines. In the most complete sections at Gacki, Leszcze and Borków this is recorded by accumulation of black, laminated clays and marls locally with numerous pelagic pteropods (*Spiratella*, J. Urbaniak, 1985) as well as tuffitic intercalations. As indicated by this fauna the refreshment was undoubtedly caused by a large influx of marine waters from the southern Paratethys (G. Czapowski, 1994). The pteropods inhabited the upper part of water body where the salinity was normal. Non-bioturbated black laminated clays indicate scarcity of bottom-living organisms and probable anoxic conditions. The basin water was density stratified similarly as before evaporation. Below pycnocline there were still incompletely diluted dense and oxygen-poor brines which were, however, unable to precipitate evaporitic minerals.

## EVOLUTION OF BASIN BRINE

Presented sedimentary history of the Nida Gypsum deposits suggests two major salinity rises both reflected by transition from the sulphate to sulphate-chloride sedimentation. The studied deposits represent thus two saline cyclothems. Several horizons with vanished halite indicate subordinate fluctuations of salinity. The first cyclothem or salinity increase (suggested also by geochemical data of A. Kasprzyk, 1994 and L. Rosell *et al.*, 1998) is recorded in the lower part of the section up to layer **ł**, the second one includes the remaining upper part of the section. The first salinity rise was interrupted by dilution accompanied with the subaqueous dissolution of previously deposited halite. The upper layer of grass-like and sabre gypsum (lithosome **F**) coincides with the beginning of second salinity rise. This rise led again to deposition of sulphates and then to mixed sulphate-chloride sedimentation. These two distinct salinity increases correlate with two cyclothems, separated by the clay lithosome **E** (B. Kubica, 1992), recognized earlier in the southern part of the basin between Cracow and Przemyśl by S. Połtowicz (1974, 1993) and other authors (see S. Kwiatkowski, 1972). Two similar cyclothems were found also at Wieliczka in Poland by J. Wiewiórka (1974) and in Ukraine by O. I. Petrichenko *et al.* (1997) and A. Poberegsky (1997).

The evolution of the basin brines during the first salinity rise can be summarized as follows. During crystallization of the giant intergrowths the volume of bottom brines was relatively low and a salinity was at the beginning of gypsum precipitation phase. Pycnocline was not at much distance from the bottom. During sedimentation of sabre gypsum the salinity of Ca-sulphate saturated brines below pycnocline was greater and closer to halite precipitation phase. The volume of bottom brines was relatively large and a pycnocline was situated near the water surface. Transition to the microcrystalline gypsum was caused by depletion of $Ca^{2+}$ and salinity increase. A salinity reached the halite precipitation phase and a brine density was maximal. Stratification of brines was more complex. The bottom brines were rich in sodium chlorides, probably anoxic and poor in $SO_4^{2-}$. The surficial oxygenated brines were $SO_4^{2-}$-rich. Common influxes of Ca-sulphate enriched brines from the other areas of the shollow basin led to gypsum precipitation due to salination effect.

Finally the sulphate-chloride brines were diluted by widespread influx of marine waters from the southern Paratethys which finished evaporative deposition in the studied area of Carpathian foreland basin.

**Acknowledgements.** The presented research was partly sponsored by the KBN grant 6 P04D 038 09. I thank G. Czapowski, A. Gąsiewicz and B. C. Schreiber for critical reading and valuable comments on earlier versions of that paper, M. Narkiewicz for editorial improvement of the text, and A. Wala for showing me his unpublished materials.

## REFERENCES


BĄBEL M. (1987) — Giant gypsum intergrowths from the Middle Miocene evaporites of southern Poland. Acta Geol. Pol., **37** (1–2): 1–20.

BĄBEL M. (1991) — Dissolution of halite within the Middle Miocene (Badenian) laminated gypsum of southern Poland. Acta Geol. Pol., **41** (3–4): 163–182.

BĄBEL M. (1992) — Rozwój facjalny, sedymentacja i diageneza gipsów nadnidziańskich. Ph.D. thesis. Arch. UW. Warszawa.

BĄBEL M. (1994) — Geneza i morfologia kryształów gipsu w badeńskich ewaporatach Ponidzia. In: Neogeńskie ewaporaty środkowej Paratetydy — facje, surowce mineralne, ekologia: 3–4. Międz. Symp. Lwów, 20–24 września 1994. Warszawa.

BĄBEL M. (1995) — Sedymentacja badeńskich gipsów Ponidzia. In: Streszczenia Referatów Wygłoszonych na Posiedzeniach Oddziału Poznańskiego PTG w 1994 r., **4**: 11–14.

BĄBEL M. (1996*a*) — Wykształcenie facjalne, stratygrafia oraz sedymentacja badeńskich gipsów Ponidzia. In: Analiza basenów sedymentacyjnych a nowoczesna sedymentologia (ed. P. H. Karnkowski): B1–B26. V Krajowe Spotkanie Sedymentologów. Warszawa.

BĄBEL M. (1996*b*) — Podmorskie rozpuszczanie halitu w badeńskich gipsach Zapadliska Przedkarpackiego. In: Analiza basenów sedymentacyjnych a nowoczesna sedymentologia (ed. P. H. Karnkowski): 52-R. V Krajowe Spotkanie Sedymentologów. Warszawa.

BĄBEL M. (1999*a*) — The roles of calcium deficiency and brine mixing in the origin of Badenian laminated gypsum deposits of Carpathian Foredeep. Intern. Symp. "Evaporates and carbonate-evaporate transitions". Abstracts. Lviv. Biul. Państw. Inst. Geol., **387**: 10–12.

BĄBEL M. (1999*b*) — Facies and depositional environments of the Nida Gypsum deposits (Middle Miocene, Carpathian Foredeep, southern Poland). Geol. Quart., **43** (4): 405–428.

BĄBEL M., BOGUCKIY A. (1999) — Basin-wide isochronic correlation of the Badenian shallow-water gypsum deposits in Ukraine, Poland and the Czech Republic. Intern. Conference "Carpathian Foredeep Basin — its evolution and mineral resources". Abstracts. Cracow. Biul. Państw. Inst. Geol., **387**: 89–90.

BĄBEL M., BOGUCKIY A., VIZNA S., YATSYSHYN A. (1999) — Reconstruction of brine paleocurrents in the Middle Miocene evaporitic basin of Carpathian Foredeep. Intern. Symp. "Evaporates and carbonate-evaporate transitions". Abstracts. Lviv. Biul. Państw. Inst. Geol., **387**: 12–13.

CZAPOWSKI G. (1994) — Sedimentation of Middle Miocene marine complex from the area near Tarnobrzeg (north-central part of the Carpathian Foredeep). Kwart. Geol., **38** (3): 577–592.

DEMARCQ G. (1989) — Nemesis and the Serravalian crisis in the Mediterranean. Ann. Géol. Pays Helléniques, Ser. I, **34** (1): 1–8.

DRONKERT H. (1985) — Evaporite models and sedimentology of Messinian and Recent evaporites. GUA, Papers of Geology, Ser. 1, **24**.

GARLICKI A. (1979) — Sedimentation of Miocene salts in Poland (in Polish with English summary). Pr. Geol. Komis. Nauk Geol. PAN, Kraków, **119**.

GEISLER-CUSSEY D. (1986) — Approche sédimentologique et géochimique des mécanismes générateurs de formations évaporitiques actuelles et fossiles. Sci. Terre, Mém., **48**.

GEISLER-CUSSEY D. (1997) — Modern depositional facies developed in evaporitive environments (marine, mixed, and nonmarine). In: Sedimentary deposition in rift and foreland basins in France and Spain (eds. G. Busson, B. C. Schreiber): 3–42. Columbia Univ. Press. New York.

KASPRZYK A. (1989) — Lithology of the Miocene sulfate deposits in the Staszów region (in Polish with English summary). Kwart. Geol., **33** (2): 241–268.

KASPRZYK A. (1991) — Lithofacies analysis of the Badenian sulfate deposits south of the Holy Cross Mts. (in Polish with English summary). Prz. Geol., **39** (4): 213–223.

KASPRZYK A. (1993*a*) — Lithofacies and sedimentation of the Badenian (Middle Miocene) gypsum in the northern part of the Carpathian Foredeep, southern Poland. Ann. Soc. Géol. Pol., **63** (1–3): 33–84.

KASPRZYK A. (1993*b*) — Gypsum facies in the Badenian (Middle Miocene) of southern Poland. Canad. J. Earth Sc., **30** (9): 1799–1814.

KASPRZYK A. (1994) — Distribution of strontium in the Badenian (Middle Miocene) gypsum deposits of the Nida area, southern Poland. Geol. Quart., **38** (3): 497–512.

KASPRZYK A. (1995) — Correlation of sulphate deposits of the Carpathian Foredeep at the boundary of Poland and Ukraine. Geol. Quart., **39** (1): 95–108.

KASPRZYK A. (1997) — Oxygen and sulphur isotope composition of Badenian (Middle Miocene) gypsum deposits in southern Poland: a preliminary study. Geol. Quart., **41** (1): 53–60.

KOWALEWSKI K. (1957) — Supplements and new data concerning the subdivision of Miocene in Poland (in Polish only). Prz. Geol., **5** (1): 1–8.

KOWALEWSKI K. (1966) — Miocène des parties de la région méridionale de Sandomierz, de Tarnobrzeg et de Chmielów–Baranów et leur rapport avec les régions avoisinantes (in Polish with French summary). Biul. Inst. Geol. (without number).

KUBICA B. (1985) — The chemical series (in Polish with English summary). In: Geology of the Tarnobrzeg native sulphur deposit (ed. K. Pawlowska). Pr. Inst. Geol., **114**: 34–54.

KUBICA B. (1992) — Lithofacial development of the Badenian chemical sediments in the northern part of the Carpathian Foredeep (in Polish with English summary). Pr. Państw. Inst. Geol., **133**.

KWIATKOWSKI S. (1972) — Sedimentation of gypsum in the Miocene of southern Poland (in Polish with English summary). Pr. Muz. Ziemi, **19**: 3–94.

KWIATKOWSKI S. (1974) — Miocene gypsum deposits in southern Poland (in Polish with English summary). Biul. Inst. Geol., **280**: 299–344.

NIEMCZYK J. (1985) — Laminated gypsum from allochthonous Miocene of the Rzeszów region (in Polish with English summary). Geol. Kwart. AGH, **11** (2): 109–119.

NIEMCZYK J. (1988) — On some aspects of gypsum lamination at Krzyżanowice near Pińczów (in Polish with English summary). Geol. Kwart. AGH, **14** (2): 75–80.

NIEMCZYK J. (1994) — Miocene pit slope failure in gypsum series from Górki near Wiślica (in Polish with English summary). Czas. Techn., Budow., **91** (2B): 70–81.

NIEMCZYK J. (1995) — Geological section at Krzyżanowice near Pińczów as a base for lithostratigraphy of the Gypsum Formation of the Nida region (Southern Poland) (in Polish with English summary). Geol. Kwart. AGH, **21** (3): 183–196.

NIEMCZYK J. (1996*a*) — On the origin of folds in the Tertiary Gypsum level in relation to olistostromes of the Carpathian foredeep (in Polish with English summary). Geol. Kwart. AGH, **22** (4): 339–357.

NIEMCZYK J. (1996*b*) — Significance of olistostromes in gypsum deposits of southern Poland (in Polish with English summary). Czas. Techn., Budow., **93** (5B): 115–129.

NIEMCZYK J. (1996*c*) — Early deformation phases of level folding as a source of effective heterogenousness in gypsum rocks around Gartatowice on Ponidzie (in Polish with English summary). Czas. Techn., Budow., **93** (5B): 130–142.

NIEMCZYK J. (1997) — Miocene slumps in the gypsum series of Siesławice near Busko Zdrój and geology of the region (Central Poland) (in Polish only). Prz. Geol., **45** (8): 811–815.

ODRZYWOLSKA-BIEŃKOWA E. (1975) — Micropaleontological stratigraphy of the Miocene of central part of the Carpathian Foredeep (in Polish with English summary). Prz. Geol., **23** (12): 597–603.

ORTÍ CABO F., PUEYO MUR J. J., GEISLER-CUSSEY D., DULAU N. (1984) — Evaporitic sedimentation in the coastal salinas of Santa Pola (Alicante, Spain). Rev. Inst. Invest. Geol., **38/39**: 169–220.

OSMÓLSKI T. (1972) — The influence of the geological structure of marginal parts of the Działoszyce Trough on the metasomatosis of gypsum (in Polish with English summary). Biul. Inst. Geol., **260**: 65–188.

OSZCZYPKO N. (1996) — The Miocene dynamics of the Carpathian Foredeep in Poland (in Polish with English summary). Prz. Geol., **44** (10): 1007–1018.

OSZCZYPKO N. (1998) — The Western Carpathian Foredeep — development of the foreland basin in front of the accretionary wedge and its burial history (Poland). Geol. Carpath., **49** (6): 415–431.

PAWLIKOWSKI M. (1982) — Mineralogical and petrographical study of alteration products of the Miocene gypsum rocks in the Wydrza sulphur deposit (in Polish with English summary). Pr. Miner. Komis. Nauk Miner. PAN, Kraków, **72**.

PERYT T. M. (1996) — Sedimentology of Badenian (middle Miocene) gypsum in eastern Galicia, Podolia and Bukovina (West Ukraine). Sedimentology, **43** (3): 571–588.

PERYT T. M., JASIONOWSKI M. (1994) — In situ formed and redeposited gypsum breccias in the Middle Miocene Badenian of southern Poland. Sed. Geol., **94** (1–2): 153–163.

PERYT T. M., KAROLI S., PERYT D., PETRICHENKO O. I., GEDL P., NARKIEWICZ W., ĎURKOVIČOVÁ J., DOBIESZYŃSKA Z. (1997) — Westernmost occurrence of the Middle Miocene Badenian gypsum in Central Paratethys (Kobeřice, Moravia, Czech Republic). Slovak Geol. Mag., **3** (2): 105–120.

PERYT T. M., JASIONOWSKI M., KAROLI S., PETRICHENKO O. I., POBEREGSKY A., TURCHINOV I. I. (1998) — Correlation and sedimentary history of the Badenian gypsum in the Carpathian Foredeep (Ukraine, Poland, and Czech Republic). Prz. Geol., **46** (8/2): 729–732.

PERYT T. M., KASPRZYK A. (1992) — Earthquake-induced resedimentation in the Badenian (middle Miocene) gypsum of southern Poland. Sedimentology, **39** (2): 235–249.

PERYT T. M., POBEREŻSKI A., JASIONOWSKI M., PETRYCZENKO O. I., PERYT D., RYKA W. (1994) — Badenian gypsum facies in the Nida and Dnister river-basins (southern Poland and SW Ukraine) (in Polish only). Prz. Geol., **42** (9): 771–776.

PETRICHENKO O. I., PERYT T. M., POBEREGSKY A. (1997) — Peculiarities of gypsum sedimentation in the Middle Miocene Badenian evaporite basin of Carpathian Foredeep. Slovak Geol. Mag., **3** (2): 91–104.

PISHVANOVA L. C. (1963) — Stratigraphical significance of foraminifera for division of the Tortonian deposits in the south-west margin of Russian Platform (in Russian). Trudy Ukrain. NIGRI, **5**: 275–291.

POBEREGSKY A. (1997) — To the question about laws of chemogenic sedimentation in the Badenian evaporite basin of the Forecarpathians. In: Abstracts of the 18th Regional European Meeting of Sedimentology, Heidelberg. Gaea Heidelbergensis, **3**: 279.

POŁTOWICZ S. (1974) — Tectonic structures of the Carpathian border in the Tarnów and Pilzno area (Polish Middle Carpathians) (in Polish with English summary). Rocz. Pol. Tow. Geol., **44** (4): 491–514.

POŁTOWICZ S. (1993) — Palinspastic paleogeography reconstruction of Badenian saline sedimentary basin in Poland (in Polish with English summary). Geol. Kwart. AGH, **19** (4): 174–178, 203–233.

PRISYAZHNIUK V. A., LUL'EVA S. A., SYABRYAJ S. V., OLSHTYNSKAYA L. V., STUPINA L. V. (1997) — New data about palaeontology and stratigraphy of the Miocene deposits of Ustechkivsky graben of Volyno-Podolia (in Ukrainian with English summary). Geol. J. (Kiev), **1–2**: 57–64.

RADWAŃSKI A. (1969) — Lower Tortonian transgression onto the southern slopes of the Holy Cross Mts. (in Polish with English summary). Acta Geol. Pol., **19** (1): 1–164.

RAUP O. B. (1982) — Gypsum precipitation by mixing seawater brines. Bull. Amer. Ass. Petrol. Geol., **66** (3): 363–367.

ROMAN A. (1998) — Wykształcenie i sedymentacja badeńskich gipsów okolic Racławic na Wyżynie Miechowskiej. M.Sc. thesis. Arch. UW. Warszawa.

ROSELL L., ORTÍ F., KASPRZYK A., PLAYÁ E., PERYT T. M. (1998) — Strontium geochemistry of Miocene primary gypsum: Messinian of SE Spain and Sicily and Badenian of Poland. J. Sed. Res., **68** (1): 63–79.

RÖGL F., STEININGER F. F. (1984) — Neogene Paratethys, Mediterranean and Indo-pacific Seaways. In: Fossils and climate (ed. P. J. Brenchley). Geol. J., Spec. Issue., **11**: 171–200. John Wiley and Sons Ltd. Chichester.

SONNENFELD P. (1984) — Brines and evaporites. Acad. Press Inc. Orlando.

SZCZECHURA J. (1982) — Middle Miocene foraminiferal biochronology and ecology of SE Poland. Acta Palaeont. Pol., **27** (1–4): 3–44.

URBANIAK J. (1985) — New data for stratigraphy of Miocene alabaster gypsum deposit at Łopuszka Wielka near Kańczuga (in Polish with English summary). Prz. Geol., **33** (3): 121–126.

WALA A. (1963) — Korelacja litostratygraficzna profili serii gipsowej obszaru nadnidziańskiego. Spraw. z Pos. Komis. PAN, Kraków lipiec–grudzień 1962: 530–532.

WALA A. (1979) — Badania litologiczne mioceńskich warstw gipsowych i ilastych z wierceń w rejonie Winiar. In: Sprawozdanie z prac badawczych mioceńskiej serii gipsowej w obszarze Niecki Nidy, zał. 4: 1–31. Arch. PG. Kraków.

WALA A. (1980) — Litostratygrafia gipsów nidziańskich (frn). In: Gipsy niecki nidziańskiej i ich znaczenie surowcowe: 5–10. Symp. nauk. Kraków.

WARREN J. K. (1982) — The hydrological setting, occurrence and significance of gypsum in late Quaternary salt lakes in South Australia. Sedimentology, **29** (5): 609–637.

WIEWIÓRKA J. (1974) — The oldest rock-salt horizon in the Wieliczka salt layered deposits (in Polish with English summary). Studia i Materiały do Dziejów Żup Solnych w Polsce, **3**: 46–58.

ZUBER A., WEISE S. M., OSENBRÜCK K., MATEŃKO T. (1997) — Origin and age of saline waters in Busko Spa (Southern Poland) determined by isotope, noble gas and hydrochemical methods: evidence of interglacial and pre-Quaternary warm climate recharges. Appl. Geoch., **12** (5): 643–660.

## HISTORIA SEDYMENTACJI BADEŃSKICH GIPSÓW PONIDZIA

Streszczenie

Na podstawie rozprzestrzenienia 5 wyróżnionych pierwotnych facji (M. Bąbel, 1999*b*), reprezentowanych przez gipsy szklicowe, rumosze kryształów gipsu, gipsy trawiaste, szablaste i mikrokrystaliczne, oraz szczegółowe interpretacje środowisk sedymentacji ich 12 subfacji (tab. I; M. Bąbel, 1999*b*), odtworzono historię sedymentacji środkowomioceńskich gipsów Ponidzia. Osady te tworzyły się w płytkim (0–5 m) basenie ewaporacyjnym. Stałe pionowe następstwo facji w dolnej części profilu: gipsy szklicowe→trawiaste→szablaste→mikrokrystaliczne, jest wynikiem spłycenia (a lokalnie wynurzenia prowadzącego do powstania rumoszy kryształów pokrywających gipsy szklicowe) i następującego po nim pogłębienia. Zmiany głębokości były stowarzyszone ze wzrostem zasolenia aż do wytrącenia halitu w gipsach mikrokrystalicznych. Wzrost zasolenia został przerwany rozcieńczeniem solanek, które wywołało rozpuszczenie wcześniej osadzonego halitu. Ponowny wzrost zasolenia wyraził się powtórzeniem sekwencji facji: gipsy trawiaste→szablaste→mikrokrystaliczne w górnej części profilu. Dolne ogniwa tej sekwencji mają zredukowaną miąższość i są obecne wyłącznie na północny badanego terenu. Wyróżnione dwa cyklotemy solne można rozpoznać na znacznym obszarze zapadliska przedkarpackiego, również na Ukrainie.

# EXPLANATIONS OF PLATES

## PLATE I

Fig. 1. Debris of gypsum crystals covering the giant intergrowths (hammer as scale, centre right). Sielec Rządowy

Fig. 2. Lower part of the Nida Gypsum deposits at Leszcze quarry. Photo by B. Kremer

## PLATE II

Fig. 1. Giant dome of sabre gypsum; 13 m in diameter, 4 m in height. Wiślica-Grodzisko

Fig. 2. Gypsum facies and subfacies at locality Chotel Czerwony–Zagórze E

## PLATE III

Fig. 1. Sabre gypsum facies at Skorocice nature reserve. Natural bridge at Wielka Góra

Fig. 2. Transition from grass-like gypsum to sabre gypsum facies at Borków quarry. Photo by A. Świerczewska

## PLATE IV

Fig. 1. Halite solution-collapse megabreccias of laminated gypsum. Leszcze quarry, farther part of the wall illustrated in Pl. V

Fig. 2. Gypsified organic mats showing empty fenestral pores (long arrows) and fenestral pores filled with coarse gypsum cement (short arrows). Borków quarry, layer **m1**. Photo by S. Ulatowski

## PLATE V

Giant-scale halite solution subsidence deformations at Leszcze quarry

## PLATE VI

Fig. 1. Upper part of the gypsum section at Borków quarry. The exposure is 13 m high

Fig. 2. Gypsum druse below the base of layer **m1** (see Pl. IV, Fig. 2). Borków quarry

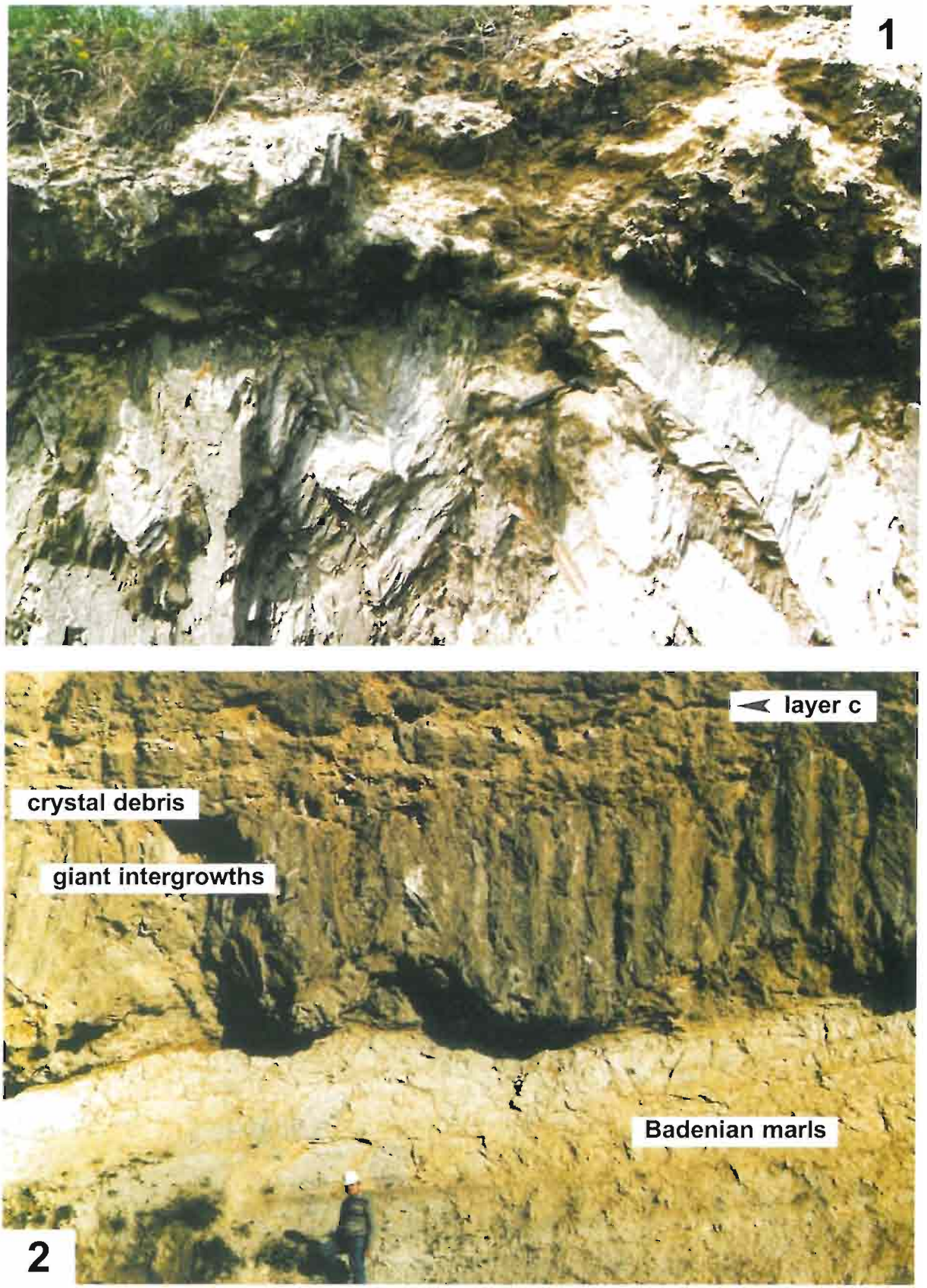


Maciej BĄBEL — History of sedimentation of the Nida Gypsum deposits (Middle Miocene, Carpathian Foredeep, southern Poland)


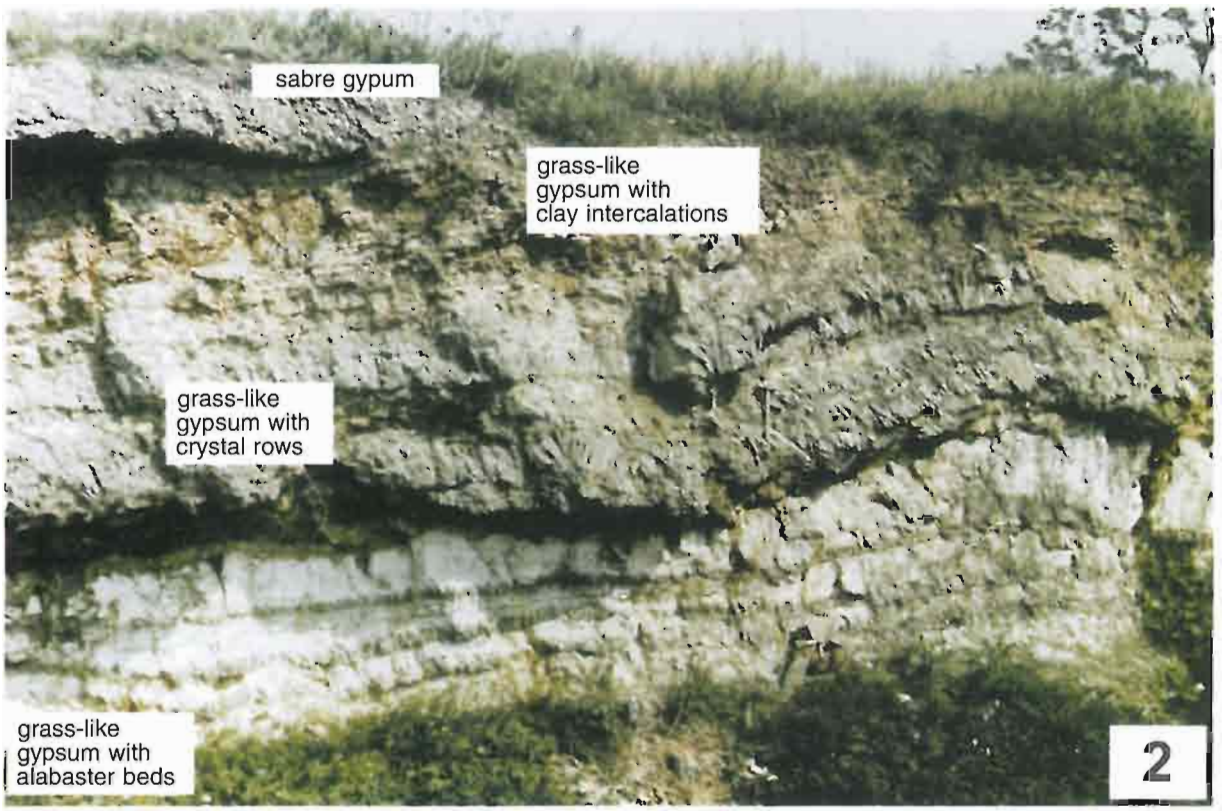


Maciej BĄBEL — History of sedimentation of the Nida Gypsum deposits (Middle Miocene, Carpathian Foredeep, southern Poland)

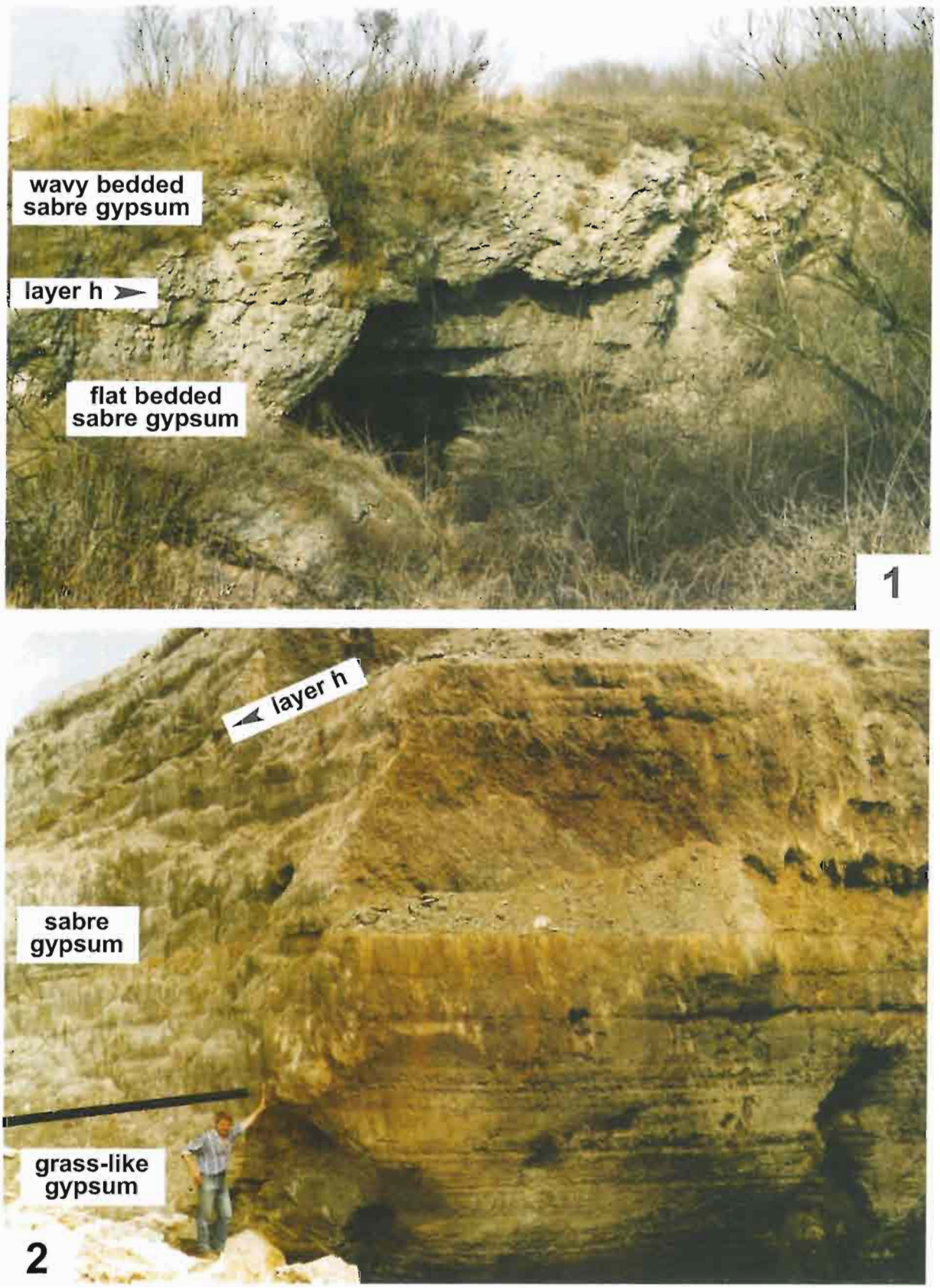


Maciej BĄBEL — History of sedimentation of the Nida Gypsum deposits (Middle Miocene, Carpathian Foredeep, southern Poland)


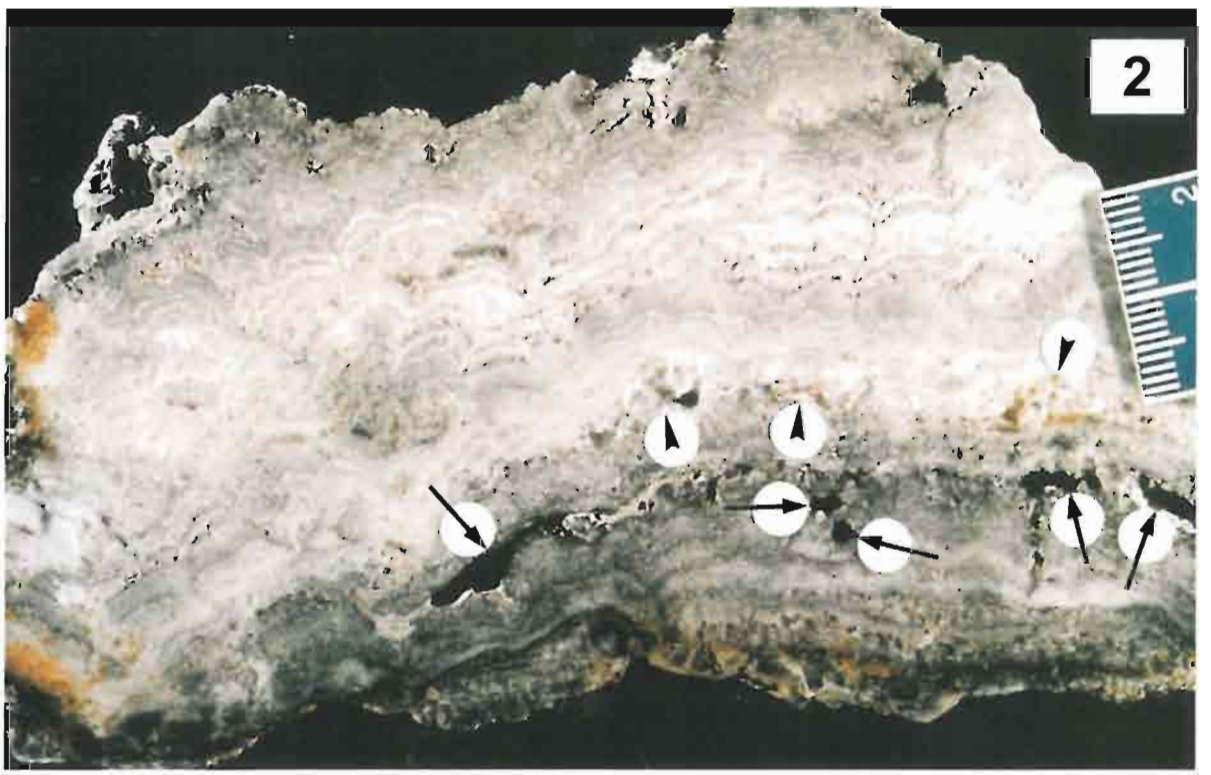


Maciej BĄBEL — History of sedimentation of the Nida Gypsum deposits (Middle Miocene, Carpathian Foredeep, southern Poland)

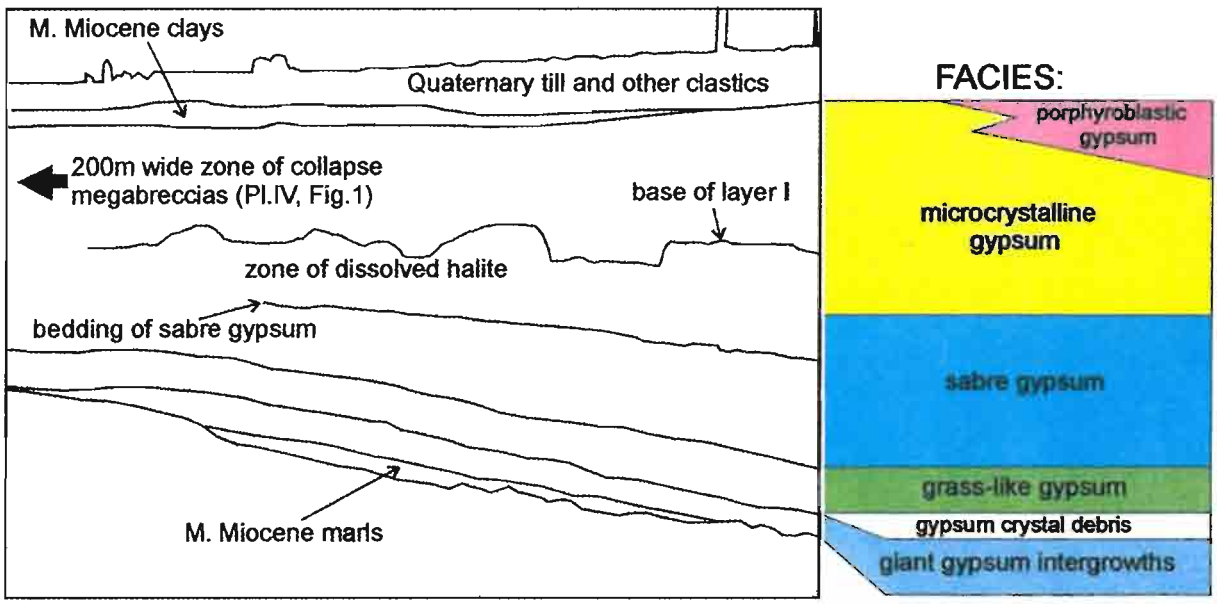
M. Miocene clays
Quaternary till and other clastics
200m wide zone of collapse
megabreccias (Pl.IV, Fig.1)
base of layer I
zone of dissolved halite
bedding of sabre gypsum
M. Miocene marls
FACIES:
porphyroblastic gypsum
microcrystalline gypsum
sabre gypsum
grass-like gypsum
gypsum crystal debris
giant gypsum intergrowths

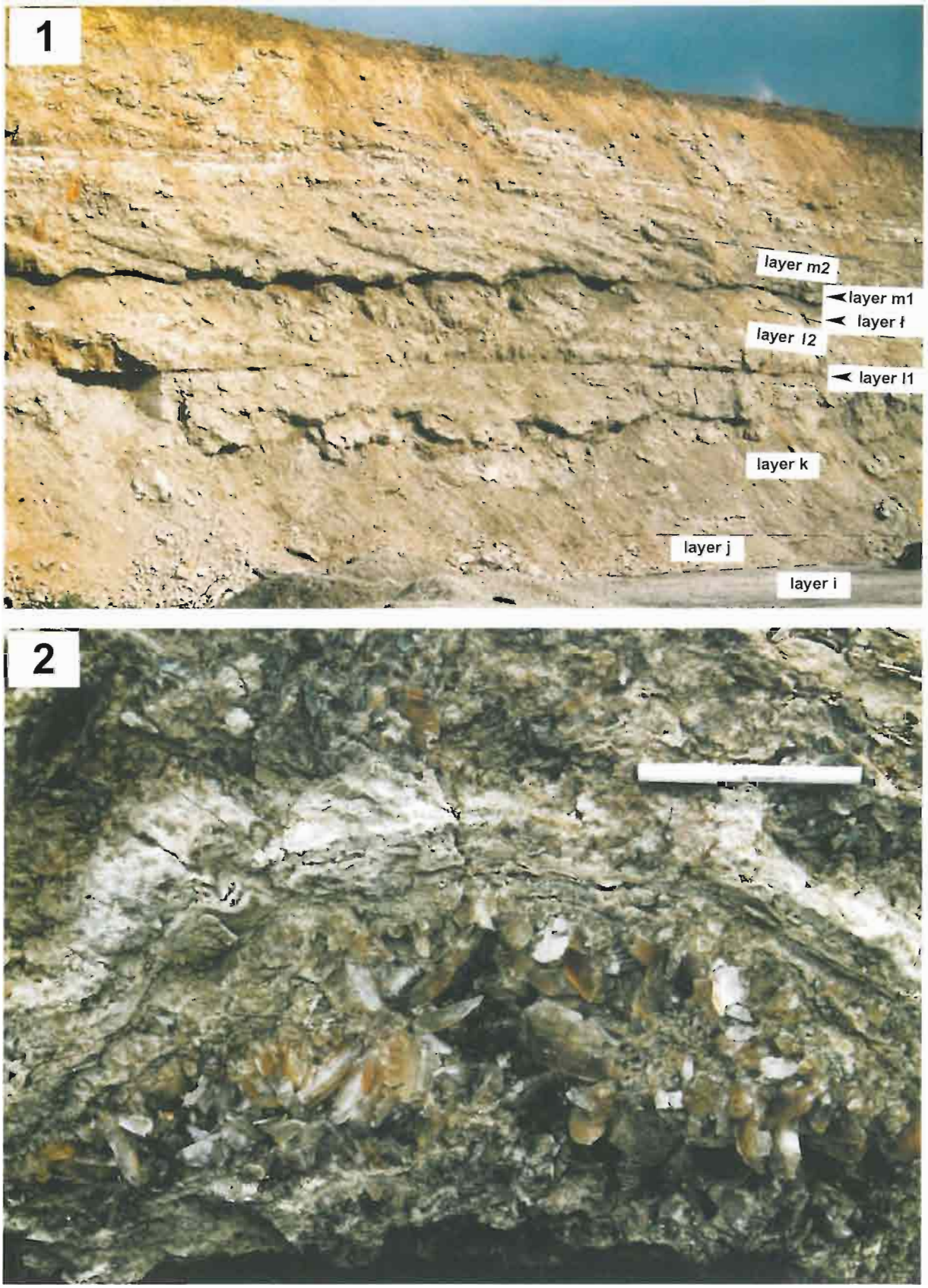


Maciej BĄBEL — History of sedimentation of the Nida Gypsum deposits (Middle Miocene, Carpathian Foredeep, southern Poland)